Oral Presentation

The 7th TSME International Conference on Mechanical Engineering
13-16 December 2016

TSME ICOME 2016
Mechanical Engineering Innovation for Green Society

DRC0003

Kinematic analysis of a 3-$\overline{P}\overline{R}RS$ Parallel Robot

Amnad Tongtib, Pinyo Puangmali and Theeraphong Wongratanaphisan*

Department of Mechanical Engineering, Faculty of Engineering, Chiang Mai University, Chiang Mai, Thailand, 50200
*Corresponding Author: E-mail: theeraphong.wong@cmu.ac.th, Telephone Number: +66-53-44146

Abstract

In this paper, kinematic analysis of a 3-$\overline{P}\overline{R}RS$ parallel robot is presented. The robot consists of a triangular moving platform connected to a rigid base through three $\overline{P}\overline{R}RS$ link chains. All three link chains are assumed identical. Each link chain composes of two rigid bodies connected in series by two actuating revolute joints. These link chains are connected to the base by prismatic joints and to the moving platform by spherical joints. The 3-$\overline{P}\overline{R}RS$ parallel robot has six degrees of freedom (DOF). It can translate the end-effector in three dimensional spaces and can provide rotational motion about three independent axes. The explicit inverse kinematic solutions are provided. The details of the steps to numerically obtain the forward kinematic solutions by dialytic elimination method are presented.

Keywords*:* parallel robot, closed-chain mechanism, kinematic analysis, dialytic elimination.

1. Introduction

In some tasks, robots are used instead of human workers because they can operate repetitively for a lengthy period of time, and in many cases, with higher accuracy. There are two types of robot structure: serial and parallel. Serial robot is an open chain of links connected in series having only one link connected to ground. Parallel robots, on the other hand, have more than one links that are connected to ground. Serial robots can cover a large working space with high degree of dexterity in the expense of large and heavy link components. Due to their structure parallel robots, comparatively, have higher stiffness and higher accuracy. The link components can be designed smaller than those of the serial type. The drawbacks are the smaller workspace and the complexity of kinematics.

The inverse kinematic of a parallel robot is generally straightforward to analyze. However, the forward kinematic can be quite complicated. The approaches to obtain solutions to the forward kinematic of a parallel robot may be divided into 3 categories: closed-form solution, numerical technique and analytical technique. For some special structure, the closed-form solutions exist. For example, the Gough platform [2,3,4] of which link components are specially symmetrically arranged such that solutions resolve into closed-form. For most other parallel robots, the closed-form solutions do not exist. A set of nonlinear equations have to be solved numerically. The methods such as Newton-Raphson[8], Global Newton Raphson [5] have been shown to obtain solutions. In analytical approach the form of equations is rearranged into other well-known form such as polynomial equations. The solutions can then be obtained from standard technique such as dialytic elimination method [9].

Generally, the working space of 6-DOF parallel robots is limited due to many constraints introduced by the nested structure of link connection. In this paper, a 6-DOF 3 legs prismatic-revolute-revolute-spherical (3-$\overline{P}\overline{R}RS$) chain parallel robot is analyzed (the overbar indicates actuating joint). With three legs, the end-effector is less restricted and hence complication is reduced which could lead to increased working space. Section 2 presents the description of the 3-$\overline{P}\overline{R}RS$ robot. In Section 3, the detail of the analytic form of inverse kinematic solutions will be explained. The procedure to obtain the forward kinematic solutions will be presented. Conclusions are provided in Section 4.

2. Description of a 3-$\overline{P}\overline{R}RS$ Parallel Robot

Fig. 1a shows the skeletal diagram of the 3-$\overline{P}\overline{R}RS$ parallel robot. It consists of a moving platform, which acts as a base holding an end-effector, connected to a fixed base through three link chains. The moving platform can be viewed schematically as a triangular plate. Each link chain consists of three rigid body connected serially by two revolute joints. These link chains are connected to the base by prismatic joints and to the moving platform at its corners by spherical joints. The revolute joints are actuating joints. The prismatic and spherical joints are passive. Let the X-Y-Z frame be a fixed frame and the x-y-z frame be attached to the moving platform. Each link chain lies on a plane which is mutually perpendicular to the planes on which the other link chains lie. Link chain 1 lies on the Y-Z plane. Its prismatic joint is along the X-axis and its two revolute joint axes are also parallel to the X-axis. This is similar for Link chain 2 to the X-Z plane and the Y-axis and Link chain 3 to the X-Y plane and the Z-axis. The end of each link chain is connected to the triangular moving platform by a spherical joint at D_i.

The degree of freedom (mobility number) of the 3-$\overline{P}\overline{R}RS$ parallel robot can be determined from

DRC0003

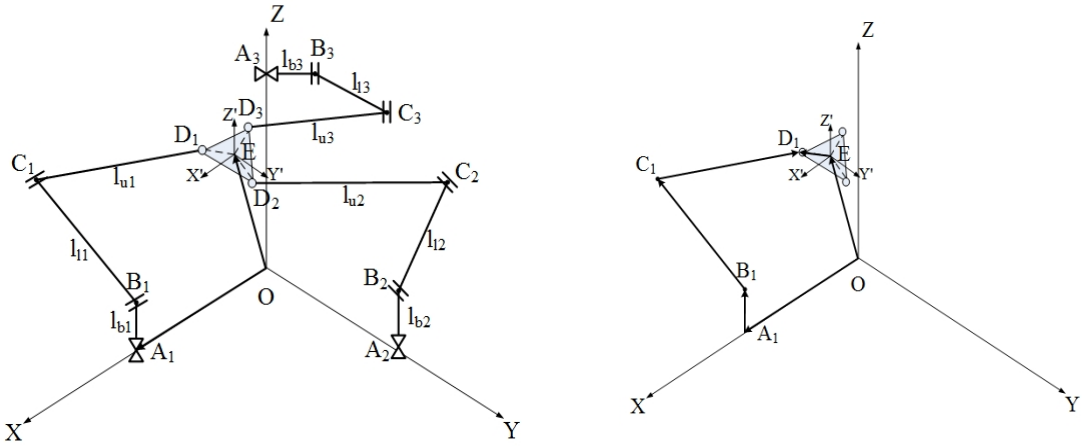

Fig. 1 a) Schematic description of a 3-$P\overline{R}\overline{R}S$ parallel robot, b) vector loop of Link chain 1 of a 3-$P\overline{R}\overline{R}S$ parallel robot

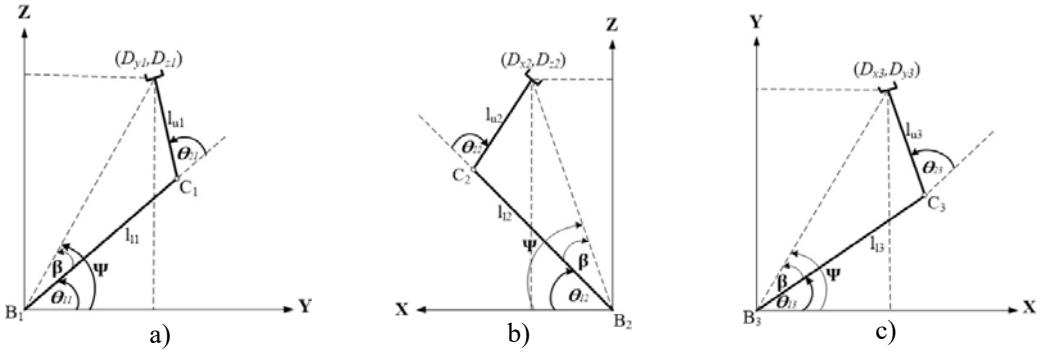

Fig. 2 Angles description of link chains

$$M = 6(n-1) - 5f_1 - 4f_2 - 3f_3, \qquad (1)$$

where

M = Degree of Freedom, D.O.F.
n = number of links (including the base)
f_1 = number of joint with 1 D.O.F.
f_2 = number of joint with 2 D.O.F.
f_3 = number of joint with 3 D.O.F.

Here, n=11, f_1 = 9, f_2 = 0 and f_3 = 3, therefore the robot has 6 degrees of freedom. This robot can perform tasks that require positioning and orientating of object(s) in three dimensional spaces.

3. Kinematic of a 3-$P\overline{R}\overline{R}S$ Parallel Robot

To analyze the kinematics of a 3-$P\overline{R}\overline{R}S$ parallel robot, consider the kinematics of a moving platform and the kinematics of each link chain. In Fig. 1b, O(0,0,0) is the origin of the fixed frame and E(e_x,e_y,e_z) is the origin of the x-y-z frame which is attached to the moving platform. Let R be the rotation matrix which maps the moving x-y-z frame onto the fixed X-Y-Z frame. For each chain i:

$$\overline{\mathrm{OD}}_i + R\overline{\mathrm{D}_i\mathrm{E}} = \overline{\mathrm{OE}}. \qquad (2)$$

Note that $\overline{\mathrm{D}_i\mathrm{E}}$ are the known local distance vectors in the rotating frame.

3.1 Inverse Kinematic

When the position E and orientation, i.e. the rotation matrix R, of the moving platform are given, the positions of all D_is can be uniquely determined. For each link chain,

$$\overline{\mathrm{OD}}_i = \overline{\mathrm{OE}} - R\overline{\mathrm{D}_i\mathrm{E}}. \qquad (3)$$

Each link chain can be considered as a 3-DOF serial planar manipulator with two actuators and one passive joint. Once the coordinate of D_i is determined, one can proceed to find the input joint angles of the actuators. Link chain 1 operates on planes parallel to the Y-Z plane. The coordinate of D_1 is (X, D_{y1}, D_{z1}) where X is long the passive prismatic joint and not directly controlled by Link chain 1. D_{y1} and D_{z1} are expressed in terms of actuating angles θ_{11} and θ_{21} (see Fig. 2a) as follow:

DRC0003

$$D_{y1} = l_{l1}\cos\theta_{11} + l_{u1}\cos(\theta_{11} + \theta_{21}) \quad (4)$$

$$D_{z1} = l_{l1}\sin\theta_{11} + l_{u1}\sin(\theta_{11} + \theta_{21}) \quad (5)$$

From Eqs. (4) and (5) the inverse kinematic solutions can be determined as

$$\theta_{21} = \tan^{-1}\left(\frac{\pm\sqrt{1-t_1^2}}{t_1}\right) \quad (6)$$

$$\theta_{11} = \tan^{-1}\left(\frac{D_{z1}}{D_{y1}}\right) - \tan^{-1}\left(\frac{l_{u1}\sin\theta_{21}}{l_{l1} + l_{u1}\cos\theta_{21}}\right) \quad (7)$$

where $t_1 = \dfrac{D_{y1}^2 + D_{z1}^2 - l_{l1}^2 - l_{u1}^2}{2l_{l1}l_{u1}}$.

Note in Eqs. (6) and (7) that for a given pair of D_{y1} and D_{z1} there exist two solutions pairs of θ_{11} and θ_{21}. Similarly, Link chain 2 and Link chain 3 operate on planes parallel to the X-Z plane and the X-Y plane, respectively. The coordinate of D_2 and D_3 are (D_{x2}, Y, D_{z2}) and (D_{x3}, D_{y3}, Z), respectively (see Figs. 2b and 2c). The corresponding relations between the input joint angles and the point Ds are

$$D_{x2} = l_{l2}\cos\theta_{12} + l_{u2}\cos(\theta_{12} + \theta_{22}) \quad (8)$$

$$D_{z2} = l_{l2}\sin\theta_{12} + l_{u2}\sin(\theta_{12} + \theta_{22}) \quad (9)$$

$$D_{x3} = l_{l3}\cos\theta_{13} + l_{u3}\cos(\theta_{13} + \theta_{23}) \quad (10)$$

$$D_{y3} = l_{l3}\sin\theta_{13} + l_{u3}\sin(\theta_{13} + \theta_{23}) \quad (11)$$

and the inverse kinematic solutions are

$$\theta_{22} = \tan^{-1}\left(\frac{\pm\sqrt{1-t_2^2}}{t_2}\right) \quad (12)$$

$$\theta_{12} = \tan^{-1}\left(\frac{D_{z2}}{D_{x2}}\right) - \tan^{-1}\left(\frac{l_{u2}\sin\theta_{22}}{l_{l2} + l_{u2}\cos\theta_{22}}\right) \quad (13)$$

$$\theta_{23} = \tan^{-1}\left(\frac{\pm\sqrt{1-t_3^2}}{t_3}\right) \quad (14)$$

$$\theta_{13} = \tan^{-1}\left(\frac{D_{y3}}{D_{x3}}\right) - \tan^{-1}\left(\frac{l_{u3}\sin\theta_{23}}{l_{l3} + l_{u3}\cos\theta_{23}}\right) \quad (15)$$

with $t_2 = \dfrac{D_{x2}^2 + D_{z2}^2 - l_{l2}^2 - l_{u2}^2}{2l_{l2}l_{u2}}$ and $t_3 = \dfrac{D_{x3}^2 + D_{y3}^2 - l_{l3}^2 - l_{u3}^2}{2l_{l3}l_{u3}}$.

Note that for the inverse kinematic problem X, Y and Z are variables that need not be determined directly. They serve to follow the constraints resulted from connecting the three link chains to the moving platform.

3.2 Forward Kinematic

An opposite problem is: 1) given the six input variables θ_{11}, θ_{21}, θ_{12}, θ_{22}, θ_{13} and θ_{23}, 2) find the three coordinates of D_is which together can be used to solve for the position of the end-effector point E and 3) the rotation matrix R. Note that D_{y1}, D_{z1}, D_{x2}, D_{z2} D_{x3}, D_{y3} can be directly determined from Eqs. (4)-(5) and Eqs. (8)-(11). The remaining steps are to find X, Y and Z. These 3 variables are related through constraints:

$$\|D_1 - D_2\| = d_1, \quad (16)$$

$$\|D_2 - D_3\| = d_2, \quad (17)$$

$$\|D_1 - D_3\| = d_3, \quad (18)$$

where d_1, d_2 and d_3 are the distances between corresponding points. Equations (16)-(18) can be rearranged as

$$k_2X^2 + k_1X + k_0 = 0, \quad (19)$$

$$m_2Y^2 + m_1Y + m_0 = 0, \quad (20)$$

$$k_5Y^2 + k_4Y + k_3 = 0, \quad (21)$$

where

$$k_1 = -2D_{x1}, k_2 = 1, k_4 = -2D_{x2}, k_5 = 1, m_1 = -2D_{y2}, m_2 = 1,$$

$$k_0 = -d_1^2 + D_{x1}^2 + D_{x2}^2 - 2D_{x2}D_{y2} + D_{y2}^2 + Z^2 - 2ZD_{z2} + D_{z2}^2,$$

$$k_3 = -d_3^2 + D_{x1}^2 + D_{x2}^2 - 2D_{x1}D_{x3} + D_{x3}^2 + Z^2 - 2ZD_{z3} + D_{z3}^2,$$

$$m_0 = -d_2^2 + D_{x3}^2 + D_{y2}^2 - 2D_{z2}D_{z3} + D_{z3}^2 + X^2 - 2XD_{x3} + D_{z3}^2.$$

Note that the coefficients k_0, k_3 are functions of Z, k_1, k_2, k_4, k_5, m_1, m_2 are constants and m_0 is a functions of X. Dialytic elimination method [9] can be used to eliminate Y and X in Eqs. (19), (20) and (21), resulting in a function of 8th-order polynomial in Z:

$$\sum_{i=0}^{8} a_i Z^i = 0, \quad (22)$$

where the coefficients a_i (i =1,2,…,8) are constants (the symbolic forms of a_i are very lengthy and their expressions are not shown here). There are maximum of 8 possible distinct solutions of Z. Once Zs are obtained X can be directly calculated from Eq. (19). Y can be obtained from Eqs. (20) or (21). Note that for each value of Z, two real values (if exist) of X and two real values (if exist) of Y can be obtained. However, the dialytic elimination procedure may produce erroneous solutions. Therefore all the obtained solutions must be checked with the original constraints (16)-(18). The maximum number of real solutions is 8. However, depending on the chosen values of θ_{11}, θ_{21}, θ_{12}, θ_{22}, θ_{13} and θ_{23} and length parameters, some solutions of polynomial equations may return complex conjugate values. In this case, the number of real solutions will be reduced. In some cases of input angles, the solution may not exist at all because the

manipulator cannot physically reach that space. Consider the following numerical examples for parameters l_{li} =400 mm, l_{ui} =450 mm, l_{bi} =0 and d_i =110 mm (i=1, 2, 3) and the input angles shown in Table 1.

Table. 1 input values for numerical examples

	θ_{11}	θ_{21}	θ_{12}	θ_{22}	θ_{13}	θ_{23}
Case 1	112.8	-101.4	86.4	-57.5	105.5	-70.3
Case 2	90.0	-90.0	88.0	-64.8	88.0	-64.8
Case 3	109.4	-125.2	99.4	-69.0	109.0	-76.3
Case 4	53.5	-31.5	56.7	-20.5	45.6	-1.3

Case 1: four solutions

In this case, the solutions for Z are 538.7, 551.2, 552.4, 695.5, 629.4±23.7j and 724.4±3.7j. There are four real solution and two complex conjugate pairs. For each real value of Z value, there exist one real values for each Y and X. Therefore, there are four solutions. The configurations corresponding to these real solutions are shown in Fig. 3.

Case 2: eight solutions

In this case, the solutions for Z are 500.0, 500.0, 500.0, 500.0, 655.0, 655.0, 655.0, 655.0. Note that all solutions for Z are real but they are repeated. There are only two distinct solutions at 500.0 and 655.0. For each real value of Z there exist 2 distinct real values for each of Y and X. The configurations corresponding to a total of eight real solutions are shown in Fig.4.

Case 3: two solutions

In this case, the solutions for Z are 555.1, 689.8, 534.3±3.1j, 622.5±104.7j, 710.6±3.3j. Here there are 2 real solutions for Z. These are substituted to solve for X and Y. When checking with the original constraints, only two real solutions exist. These configurations are shown in Fig.5. Note that in these configurations, the edge connecting points 1 and 2 are on the plane parallel to the X-Y plane.

Case 4: one solution

In this case, the solutions for Z are 600.0, 600.0, 506.8±9.2j, 600.0±131.2j, 693.3±9.2j. There are repeated real solutions at 600.0. After finding X and Y, it turns out that only one solution exists. This solution corresponds to the configuration where the end effector plate is parallel to the X-Y plane as shown in Fig.6.

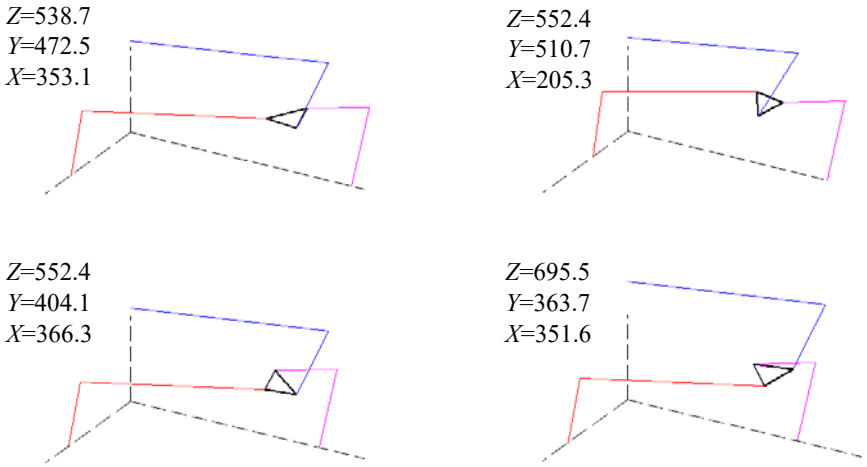

Fig. 3 Forward kinematic solution for case 1 (four solutions)

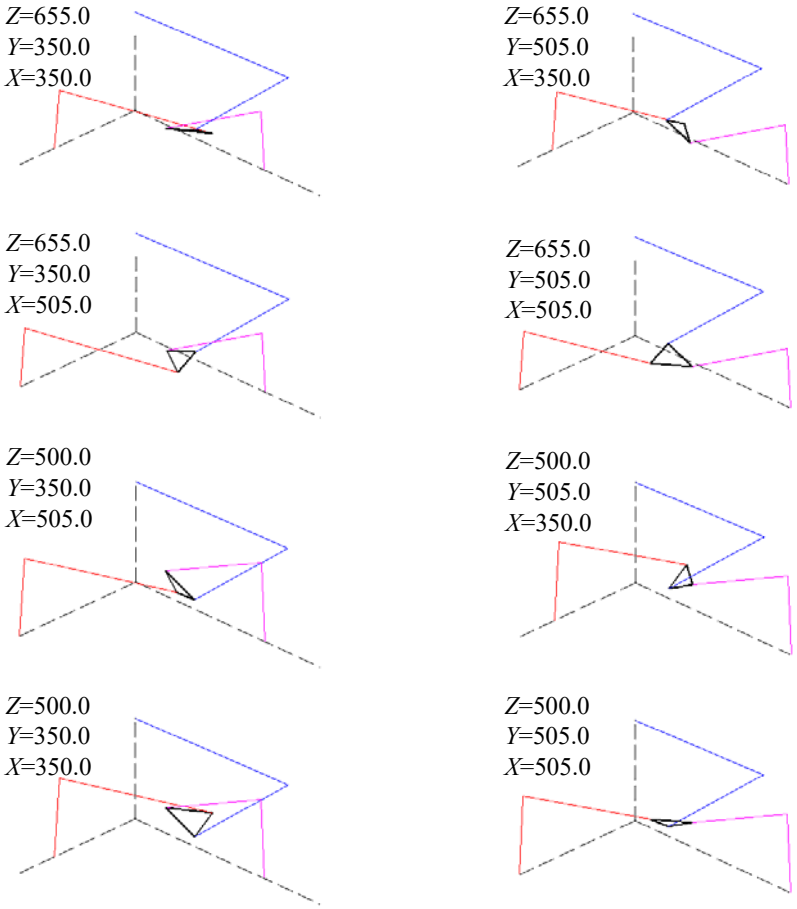

Fig. 4 Forward kinematic solution for case 2 (eight solutions)

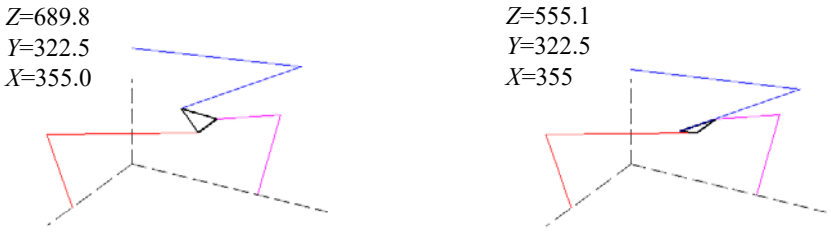

Fig. 5 Forward kinematic solution for case 3 (two solutions)

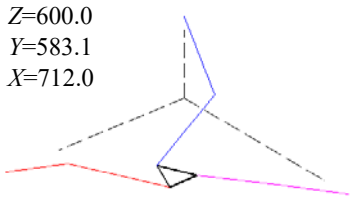

Fig. 6 Forward kinematic solution for case 4 (one solution)

From the examples above, case 1 corresponds to general configurations where the plane of the end-effector or the line representing the edge is not parallel to the plane X-Y or Y-Z or X-Z and the end-effector is well within the reachable workspace of the robot. Case 2-4 are special cases in terms of geometry. Case 2 is where the all three passive lines intersect at one point creating special symmetry. Similarly, case 3 is where two passives lines (in this case along x and y) intersect. Therefore the line connecting corner 1 and 2 of the end-effector are in the plane parallel to X-Y plane. Case 4 is where the three lines are distanced apart close to the side length of the end-effector. This corresponds to the configuration where the robot is at the boundary of the reachable workspace.

4. Conclusions

In this paper, a 6-DOF 3-$P\overline{R}\overline{R}S$ parallel robot is introduced and kinematic analyses are provided. The inverse kinematic can be obtained straightforwardly. For a given end-effector position and orientation, there exist 2 configurations of each link chain accounting for a total 8 inverse kinematic solutions. The forward kinematic solutions of this mechanism can be obtained through dialytic elimination method. In general, there are 4 forward kinematics solutions. However at a special configuration where all three passive lines intersect at one point there can be a maximum of 8 real solutions. The number of real solutions will be reduced to 2 when one of the edges of the end-effector is parallel to one of the passive planes. Furthermore only one solution exists when the end-effecor plane is parallel to one of the passive planes.

5. Acknowledgement

This work is partially supported by 1) Mid-Career Researcher Grant, Chiang Mai University and 2) the Center Mechatronic System and Innovation, Chiang Mai University.

6. References

[1] Gosselin, C. (1990). Determination of the Workspace of 6-dof parallel manipulators, *ASME J. of Mechanical Design*, vol.112(3), September 1990, pp. 331-336.

[2] Ping, J. (2001). A closed-form forward kinematics solution for the 6-6 Stewart platform, *IEEE Transaction, Robotics and Automations*, vol.17(4), August 2001, pp.522-526.

[3] Kai, L., Fitzgerald, J.M. and Lewis, F.L. (1993). Kinematic analysis of a Stewart platform manipulator, *IEEE Transaction, Industrial Electronics,* vol.40(2), April 1993, pp.283-293.

[4] Xiguang, H. and Guangpin, H. (2009). Closed-form direct position analysis of the general Stewart-Gough manipulator robot, *Mechatronics and Automation*, paper presented in the *ICMA International Conference 2009*, Changchun, China.

[5] Chifu, Y., Huang, Q., Ogbobe, P.O. and Han, J. (2009). Forward kinematics analysis of parallel robot using global newton-raphson method, *Intelligent Computation Technology and Automation*, paper presented in the *Second International Conference 2009*, Changsha, Hunan, China.

[6] Yuan, Y., Liping, W and Liwan, G. (2004). Dimensional synthesis of a 3-dof parallel manipulator, system, *Man and Cybernetics*, paper presented in the *IEEE International Conference 2004*, The Hague, Netherlands.

[7] Gosselin, C. (1988). Kinematic analysis optimization and programming of parallel robotic manipulator, McGill University, Canada.

[8] Merlet, J. P. (2006). Parallel Robots (Solid Mechanics and Its Applications), Springer-Verlag New York, USA.

[9] Tsai, L. W. (1999). Robot analysis and Design: The Mechanics of Serial and Parallel Manipulators, John Wiley & Sons, USA.